ROTATIONAL CAPACITY OF REINFORCED CONCRETE BEAMS

Arne Hillerborg
Div. of Building Materials, Lund Inst. of Tech.
Professor

ABSTRACT

The rotational capacity of a plastic hinge is analysed by means of a new approach, where the strain localization in the compression zone is taken into account. This leads to a strong size dependency of the rotational capacity. Comparisons with test results confirm this conclusion.

Key-words: Rotational capacity, limit design.

1. INTRODUCTION

Where limit design is used for reinforced concrete structures, this is based on the theory of plasticity. Before the ultimate limit state is reached, a moment redistribution is assumed to take place. Plastic hinges are assumed to be formed, which enable the moment redistribution.

Limit design is only acceptable if the plastic hinges are able to undergo a sufficient plastic rotation without loosing their bending (or shear) strength. The possible plastic rotation without a strength loss is called the rotational capacity.

In limit analysis the necessary plastic hinge rotations for the assumed moment redistribution can be calculated and compared to the rotational capacities.

Formulas or diagrams for the calculation of rotational capacities are given in some design codes, e.g. the CEB Model Code /1/. These are based on extensive tests. A review of tests and values has recently been given by Langer /2/.

In earlier studies of rotational capacities, the beam depth has never been regarded as an important parameter for beams with the same size proportions and the same reinforcement ratios. The present paper will concentrate on the influence of the beam depth.

2. DEFINITION OF ROTATIONAL CAPACITY

In test reports the rotational capacity is mostly defined as the plastic hinge rotation at maximum bending moment.

In design, the bending moment capacity is generally calculated with respect to the yield strength of the reinforcement. When the maximum bending moment is reached in a test, the steel stress is normally higher than the yield strength, which means that the bending moment is higher than the design moment for the hinge section. From the point of view of safety it seems to be sufficient that the remaining bending moment capacity, after the plastic hinge rotation has taken place, is at least as high as the design moment capacity. Thus also a plastic hinge rotation, which is larger than the rotation at maximum moment, ought to be acceptable, provided that the moment capacity has not fallen below the design moment.

In the theoretical analysis below it has been assumed that the rotational capacity is reached when the strain in the reinforcement starts decreasing. When this happens the bending moment starts to descend sharply.

The main reason why this definition has been chosen is that the simplified assumption of an elastic-perfectly plastic stress-strain curve for the reinforcing steel leads to unrealistic results if the maximum point in the moment-curvature diagram defines the rotational capacity, see below. For real, strain-hardening, steel qualities the difference in definitions is of a minor importance.

3. ANALYTICAL MODEL

3.1 Concrete stress-strain curve in compression

Within the research on fracture mechanics of concrete it has been generally accepted that the behaviour of concrete in tension cannot be described by means of only a stress-strain diagram. A pure stress-strain diagram can only be used for strains which are smaller than the strain at maximum stress, i.e. for the ascending branch and corresponding unloading branches. The descending branch is always accompanied by a strain localization to a damage zone (also called fracture zone or process zone). An additional deformation is localized to this zone, which has a limited length in the stress direction (of the order of the maximum aggregate size). The material outside this zone is unloaded. The properties of the damage zone have to be described by means of a stress-displacement curve, showing the relation between the additional deformation within the damage zone, and the corresponding stress, which is transferred through this zone.

The same idea may also be applicable to the behaviour in compression, even though this behaviour is much more complicated than in tension. Tensile failure can take part without any lateral strains and stresses, and a one-dimensional description of the behaviour is reasonably realistic. This one-dimensional property can be determined in a tensile test.

Compression failure is always accompanied by lateral strains. These strains may cause a complicated three-dimensional state of stress, particularly where the concrete is confined. The confinement may be due to stirrups, to ajoining concrete, to external forces etc. The stress-deformation properties in the main compressive stress direction depends on this confinement. These properties cannot be determined by means of a simple one-dimensional test.

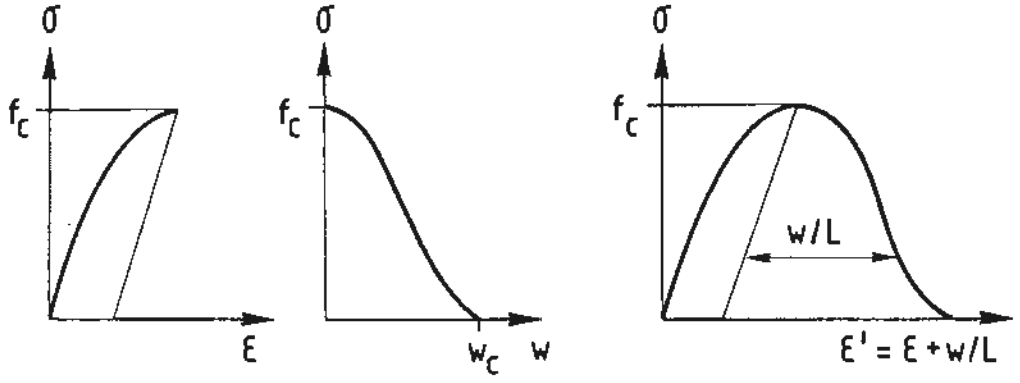

Fig. 1. The description of the stress-deformation relation by means of two diagrams.

In spite of these complications it may be possible to describe the properties in compression by means of the same types of diagrams as in tension, i.e. a stress-strain curve for the ascending branch and a stress-displacement curve for the descending branch, Fig. 1. The total deformation ΔL within a length L is then given by

$$\Delta L = \epsilon L + w \qquad (1)$$

where ϵ and w are taken from the two diagrams for the same value of the stress σ. When a damage zone has started to develop, the material outside this zone is unloaded, which means that ϵ in this case is the value from the unloading branch.

Eq. (1) can be transformed into an average strain ϵ' on the length L

$$\epsilon' = \epsilon + w/L \qquad (2)$$

and a corresponding stress-strain diagram can be calculated. Such a diagram may be used for an approximate analysis of the stresses in the compression zone of a bent beam.

In order to apply Eq. (2), it is necessary to introduce a value of L, which is the length over which the localized additional deformation w of the damage zone should be averaged. It is assumed that this length is proportional to the depth x of the compression zone

$$L = \beta x = \beta \xi d \qquad (3)$$

where β is a proportionality factor, which probably is of the order 0.8 for a rectangular beam, d is the effective depth of the beam and ξ is the relative depth of the compression zone, $\xi = x/d$.

For the numerical analysis it has been assumed that the ascending branch has the shape of a parabola with a strain at maximum equal to ϵ_o, Fig. 2.

The descending branch is in practice only of interest down to a stress of approximately $f_c/2$, where f_c is the compressive strength. This part of the curve is sufficiently well described by means of a parabola. This gives the complete stress-strain curve according to Fig. 2.

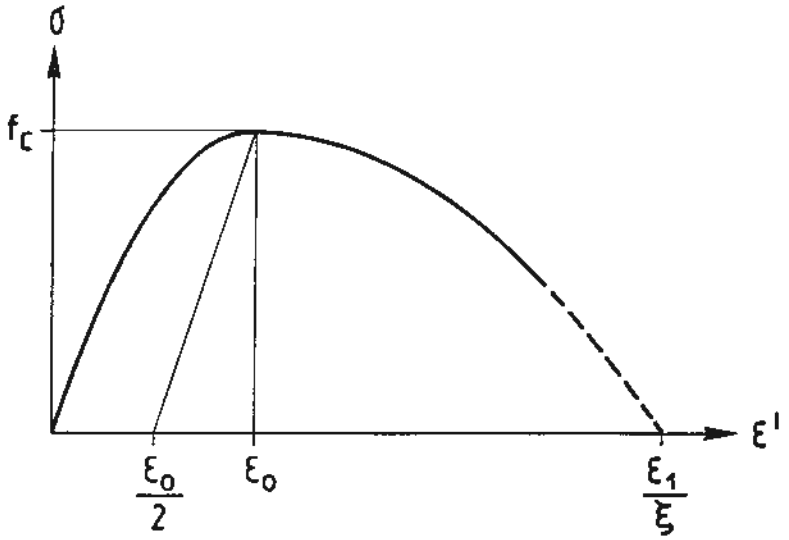

Fig. 2. Assumed parabolic shape of the formal stress-strain relation on length L, used in the numerical analysis.

The curve reaches zero stress for a strain, which is denoted ϵ_1/ξ. According to Eq. (2) this strain ought to be

$$\epsilon_o/2 + w_c/L \qquad (4)$$

with w_c defined as the additional deformation within the damage zone when the stress reaches zero, cf. Fig. 1. As an approximation, which simplifies the analytical expressions, it is assumed that the first term of Eq. (4) is small compared to the second term, and thus can be deleted. We then find

$$\epsilon_1/\xi = w_c/L \qquad (5)$$

and, by application of Eq. (3)

$$\epsilon_1 = w_c/(\beta d) \qquad (6)$$

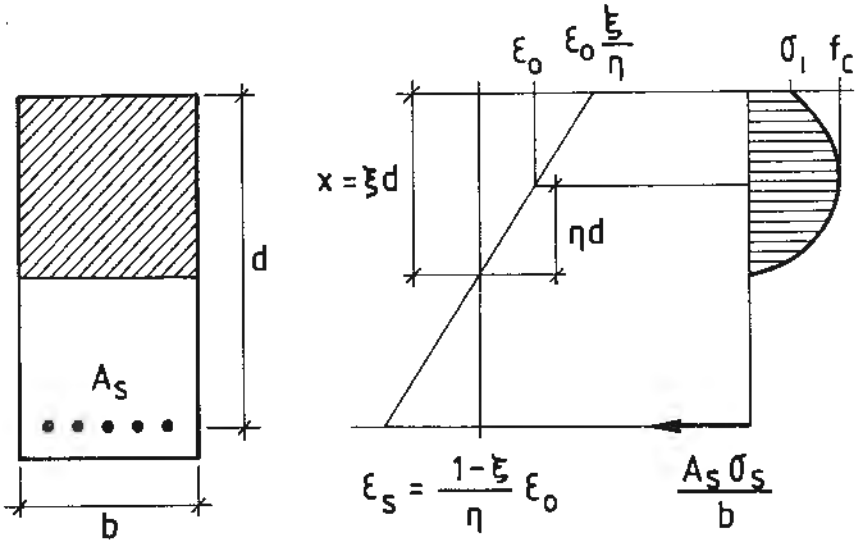

Fig. 3. Assumed strains and stresses in a rectangular beam section.

3.2 Analysis of a rectangular section

Fig. 3 shows the strains and stresses in a rectangular beam with tension reinforcement in the cracked stage. The strain distribution has been assumed to be linear, which corresponds to the ordinary assumption that plane sections remain plane. This is of course a rather rough approximation, but it is in accordance with general design practice. With the notations of the figure the following strain relations can be found

$$\varepsilon_s = \frac{1-\xi}{\eta} \cdot \varepsilon_0 \tag{7}$$

From the stress-strain curve in Fig. 2 and the strain distribution of Fig. 3, the following relation can be found

$$\frac{\sigma_1}{f_c} = 1 - \left[\frac{\frac{\xi}{\eta} - 1}{\frac{\varepsilon_1}{\xi \varepsilon_0} - 1} \right]^2 \tag{8}$$

Equilibrium of horizontal forces gives, after simplifications,

$$\frac{A_s \sigma_s}{b d f_c} = \frac{2}{3}\xi + \frac{1}{3} \cdot \frac{\sigma_1}{f_c}(\xi - \eta) \tag{9}$$

Moment equilibrium with the acting bending moment M gives

$$\frac{6M}{b d^2 f_c} = \xi\left(4 + \eta - \frac{5}{2}\xi\right) + \frac{\sigma_1}{f_c}(\xi - \eta)\left(2 - \frac{1}{2}(\xi - \eta)\right) \tag{10}$$

The curvature is

$$\frac{1}{r} = \frac{\varepsilon_0}{\eta d} \tag{11}$$

The above equations are valid after the strains in the extreme fiber of the compression zone have exceeded ε_0. For smaller strains the corresponding expressions are trivial, and need not to be shown here.

3.3 Some applications

3.3.1 Elastic-perfectly plastic reinforcement

The simplest possible stress-strain curve for the reinforcement is according to Fig. 4, without strain hardening after the yield strength has been reached. This curve is not quite realistic, but because of its simplicity it may form a basis for numerical applications.

The following material properties have been assumed in the numerical application:

$\epsilon_o = 0.002$
$f_s^o = 400$ MPa
$E_s = 200$ GPa

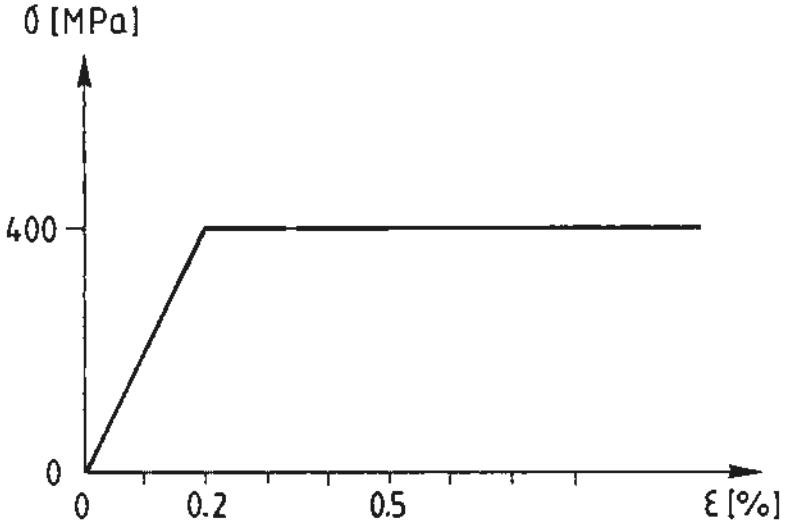

Fig. 4. Elastic-perfectly plastic stress-strain curve for the reinforcing steel.

The values of ϵ_1 and of the mechanical reinforcement ratio

$$\omega = \frac{A_s f_s}{bdf_c} \qquad (12)$$

have been varied in the analyses.

Examples of results of the analyses are shown in Fig. 5 as relations between bending moments and curvatures, in both cases as dimensionsless numbers.

It can be seen that the shapes of the curves are strongly dependent on the value of ϵ_1, which in its turn is inversely proportional to the beam depth d, see Eq. (6). Particularly the point on the curves, where the moment starts decreasing sharply, is influenced by the beam depth d. This point is where the reinforcement strain stops increasing, and starts decreasing. It thus corresponds to the situation, which above has been used to define the rotational capacity.

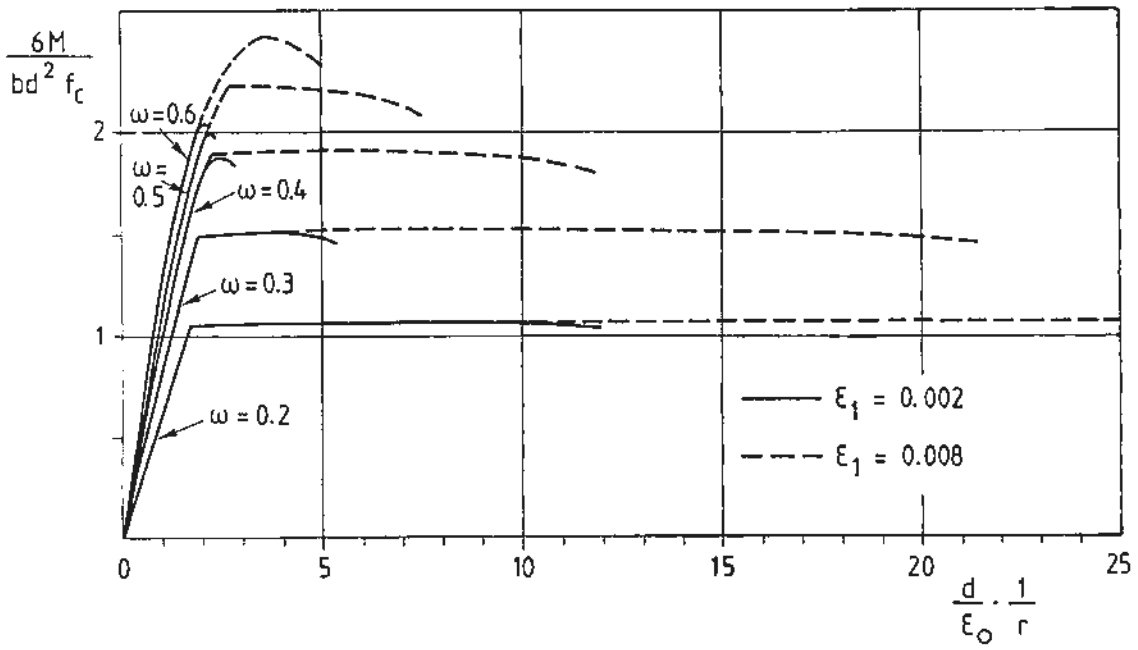

Fig. 5. Examples of theoretical moment-curvature relations with assumptions according to Figs. 2-4.

With this definition the bending moment, when the rotational capacity is reached, is in this case somewhat smaller than the maximum moment, which is approximately equal to the design moment. The difference is only of the order of 5 %. The strain hardening of real reinforcement qualities will normally cancel this difference, as will be demonstrated in the next paragraph.

The angle of rotation corresponding to the curvature in Fig. 5 can be calculated as the curvature times the length, for which this curvature is valid. This length can be assumed to be equal to the length L, over which the localized additional deformation in the compression zone is averaged, Eq. (3). With curvature from Eq. (11) and β from Eq. (6), the angle of rotation θ then is

$$\theta = \frac{L}{r} = \frac{\beta\xi d\varepsilon_0}{\eta d} = \frac{\beta\xi\varepsilon_0}{\eta} = \frac{\xi\varepsilon_0 w_c}{\eta\varepsilon_1 d} \qquad (13)$$

The most interesting value of θ is the value θ_{max}, corresponding to the definition of rotational capacity. This value can be be numerically calculated from Eq. (13) for each combination of material properties.

An analysis of the results of such calculations reveals that θ_{max} can approximately be written

$$\theta_{max} = \frac{0.6 w_c}{\omega d} \qquad (14)$$

with an accuracy of about 10% for all normal combinations of properties.

Θ_{max} according to Eq. (14) can in most cases be taken as a measure of the rotational capacity. However, the rotational capacity by definition is only the plastic hinge rotation, whereas Θ_{max} includes also a certain elastic deformation angle. By using Eq. (14) the rotational capacity may be overestimated, particularly where Θ_{max} is small, i.e. for heavily reinforced sections. Some kind of correction for the elastic part of the angle should thus be used.

The elastic part of the curvature corresponds approximately to the stage when the stress in the reinforcement reaches the strength f_s. Then the steel strain is $\epsilon_s = f_s/E_s$, and the curvature

$$(\frac{1}{r})_{el} = \frac{1}{(1-\xi)d} \cdot \frac{f_s}{E_s} \qquad (15)$$

according to Fig. 3. The elastic part of the rotation on length L according to Eq. (3) is then

$$\Theta_{el} = \frac{\beta\xi}{1-\xi} \cdot \frac{f_s}{E_s} \qquad (16)$$

For the cases where the rotational capacity is of interest, the relative depth ξ of the compression zone cannot be expected to be greater than about 0.5. The value of β is of the order 0.8. Thus a value on the safe side for Θ_{el} seems to be

$$\Theta_{el} = \frac{f_s}{E_s} \qquad (17)$$

With this approximation, the rotational capacity, i.e. the plastic hinge rotation, can be written

$$\Theta_{pl} = \Theta_{max} - \Theta_{el} = \frac{0.6w_c}{\omega d} - \frac{f_s}{E_s} \qquad (18)$$

3.3.2 Strain-hardening reinforcement

The assumption of elastic-perfectly plastic reinforcement according to Fig. 4 is not realistic, as all real reinforcement qualities show strain hardening.

Fig. 6 shows an example of a stress-strain curve for mild reinforcing steel. By means of this curve the moment-curvature relations have been evaluated with the formulas above. The results are shown in Fig. 7. From this figure it is evident that the moment increases above the design moment, which corresponds to the moment at the breakpoint, and that the moment when the rotational capacity is reached is higher than the design moment. This confirms what was stated above.

The analytical expressions are based on the assumption that plane sections remain plane. For late deformation stages this is

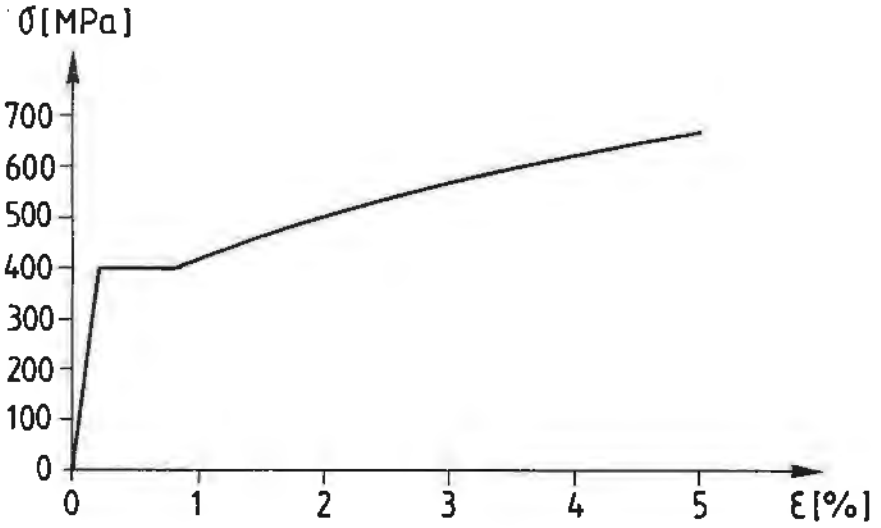

Fig. 6. Strain-hardening stress-strain curve for the reinforcing steel.

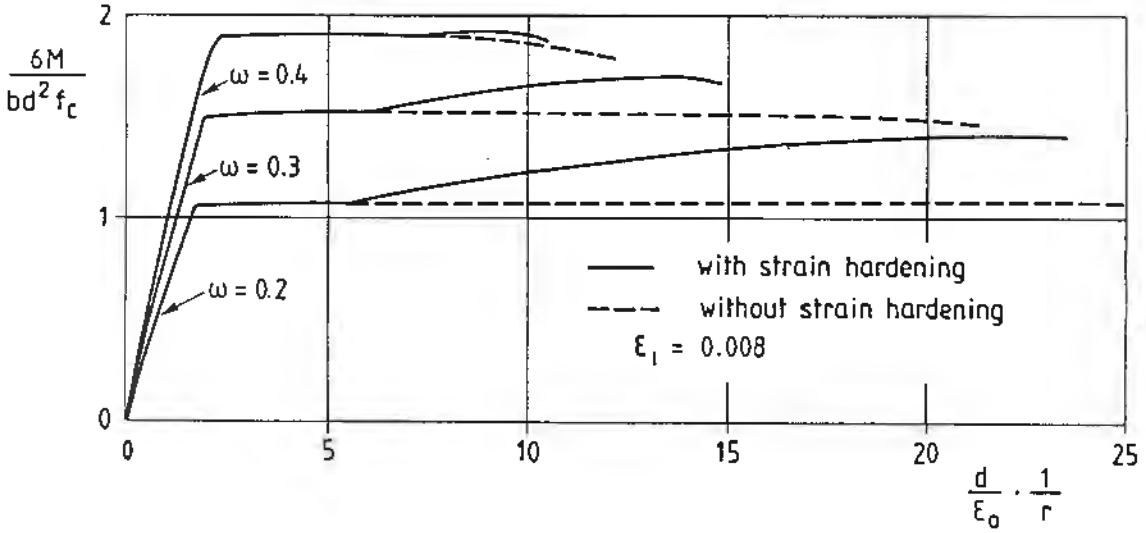

Fig. 7. Examples of theoretical moment-curvature relations with an assumed curve according to Fig. 6.

not true for sections close to supports, where skew cracks are formed. Thus the reinforcement on a certain length on both sides of the support has a nearly constant stress, rather than a stress which follows the theoretical moment distribution. The result is smaller steel strains than according to the assumption of plane sections. The steel strains will not reach the values assumed in the analysis, but only a certain portion of these values. For strain hardening steel the stresses will not reach the formally calculated stresses. Therefore the curves in Fig. 7 exaggerate the influence of strain hardening. The truth lies somewhere between the curves in Figs. 5 and 7.

4. COMPARISONS WITH TEST RESULTS

The most striking thing with the theoretical Eq. (18) for rotational capacity is the large dependence on the beam depth d.

Such a dependence has never before been reported. It is therefore necessary to compare the theoretical conclusion with test results. It is then important to use test series with large variations in beam depths for the comparison. Only one report has been found, which fulfils this requirement, viz. the tests by Corley /3/. In his tests the beam depth varied from 5 to 30 inches, i.e. with a factor of 6.

Beside the variation of beam depth and reinforcement ratio, Corley also varied other factors, like the amount of stirrups, compression reinforcement, and span to depth ratio. These factors also have an influence on the rotational capacity, which will be discussed below. To begin with we neglect all these factors and take only the properties of Eq. (18) into account. One exception is however the compression reinforcement. As value of the mechanical reinforcement ratio the difference between the mechanical reinforcement ratios of the tension (ω) and compression (ω') reinforcements has been used.

Corley reports the rotational capacity as a value θ_{tu}, which corresponds to half the rotational capacity θ_{pl} above. Thus the value of θ_{pl} used in the comparison is equal to $2\theta_{tu}$.

In order to show the influence of the beam depth d, Eq. (18) has been rewritten

$$(\theta_{pl} - \frac{f_s}{E_s})(\omega-\omega') = \frac{k}{d} \qquad (19)$$

where k should be a constant, corresponding to $0.6w_c$, if the theoretical expression is valid.

Fig. 8 shows the relation between the left hand side of Eq. (19) and 1/d. Those of Corley's beams, which showed a shear fracture, were excluded from the comparison. These same beams were also excluded by Corley in his own treatment of the results.

Fig. 8 clearly shows that Eq. (19) reasonably well describes the test results, and that the beam depth is an important factor. If the beam depth had not had any influence, the results should have been better described by means of a horizontal line.

The mean value of k from Corley's tests is 0.124 in = 3.1 mm, with a coefficient of variation of 0.40. This coefficient of variation is not high, taking into account that many influencing factors have been neglected.

Corley in his report also mentioned that the size of the member might be important for the rotational capacity. In his test evaluation he however mainly attributed the greater rotational capacities of the smaller beams to their higher content of stirrups. As will be discussed below, the high amount of stirrups in the small beams can hardly have had such a great influence on the rotational capacities. Corley, in his proposed formulas had a certain size influence, but it is much smaller than the influence according to Eq. (18).

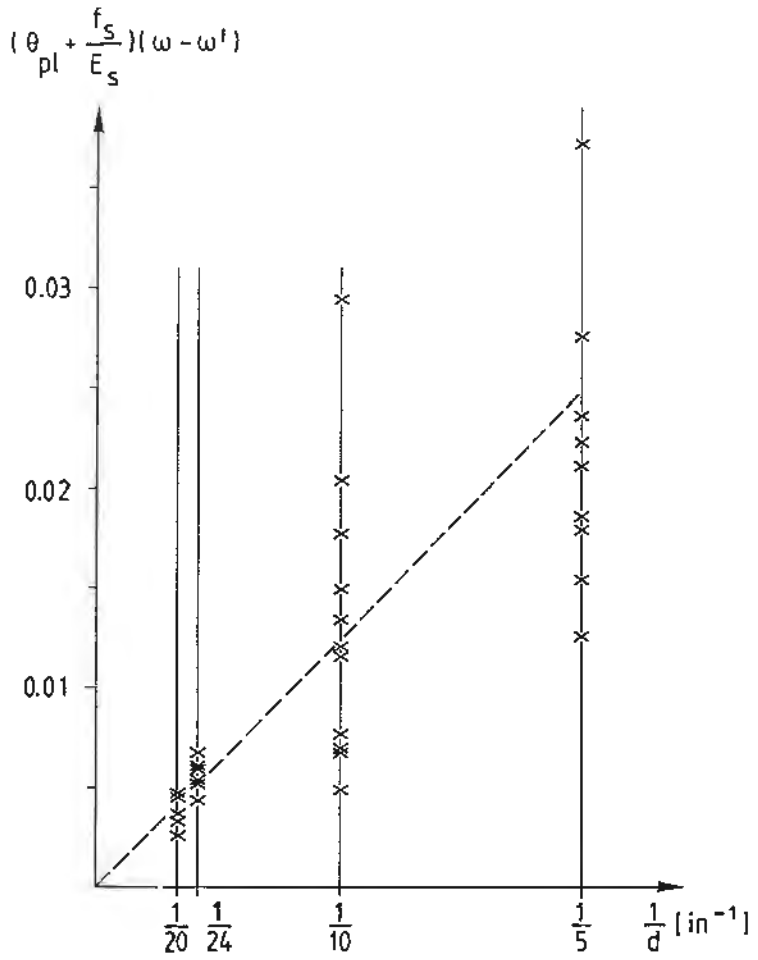

Fig. 8. Evaluation of test results according to Corley /3/.

5. OTHER INFLUENCING FACTORS

As has been pointed out above, many factors may be expected to influence the rotational capacity, beside those included in Eq. (18). These will be discussed below.

5.1 Span to depth ratio

The span to depth ratio (or better M/Vd) has certainly some influence on the rotational capacity. When this ratio increases, some distributed plastic curvature outside the localized zone will increase the rotational capacity. From Corley's tests it looks like the rotational capacities were increased in the order of 20% when the span was doubled. This influence is small, compared to the influence of the beam depth.

5.2 Compression reinforcement

The compression reinforcement corresponds theoretically to an increase in the strength of the compression zone. This influence has been taken into account in the treatment of the test in Fig. 8 by subtracting the mechanical reinforcement of the compression reinforcement from the mechanical reinforcement of the tension reinforcement.

Compression reinforcement can however also have a negative effect on the rotational capacity, viz. if it buckles before the deformability of the compression zone has been utilized. The risk of buckling depends on concrete cover, on stirrups, on bar size, and on the straightness of the reinforcing bars. Buckling has not been reported by Corley.

Compression reeinforcement can also have a positive effect for the confinement of the concrete, provided that it is kept in position by a sufficient amount of stirrups.

5.3 Stirrups

Stirrups can influence the rotational capacity in many ways. It has already been mentioned that they are essential for preventing buckling of the compression reinforcement.

The most important influence of stirrups on the rotational capacity is mostly believed to be as confining reinforcement for the concrete in the compression zone. In order to be effective from that point of view the stirrup spacing must be sufficiently small, and the stirrups must be outside most of the compression zone.
The compressive failure of concrete takes place in a zone, which has a length in the span direction equal to or smaller than the depth of the compression zone. In order to be efficient as confinement, the stirrup spacing ought not to be greater than the depth of the compression zone at failure. It can be demonstrated that the spacing is larger than this in many of Corley's beams, particularly in the 5 in beams. The confinement can then be doubted.

The concrete cover to the longitudinal reinforcement in all Corley's beams was 5/8 in. For the 5 in. beams the theoretical depth of the compression zone at failure varied beween about 1 and 3 in. For the low values of compression zone depth less than half of the zone was inside the stirrups, and in this case there can hardly be any confinement. For the highest values of the compression zone depth about 80% of the compression zone was inside the stirrups, but still the highest stressed 20% were outside, and the confining effect can be doubted.

The 5 in. beams had the highest ratios of stirrup reinforcement. Due to the reasons given above, the influence of the stirrups on the rotational capacities may be expected to be small or negligible for these beams. A study of the variation in rotational capacities with the amount of stirrups for these beams verifies this conclusion.

For the larger beams a certain increase in rotational capacities with an increase in the amount of stirrups can be seen in the tests. The results are however difficult to interpret, and they show a great scatter.

It should also be mentioned that stirrups may influence the strain distribution in the tension reinforcement, as they decrease the inclination of the skew cracks. In this way the stress and strain in the reinforcement at the support increases, and more of the strain hardening of the reinforcing steel may develop.

5.4 Type of reinforcement

The type of reinforcement may be expected to have an influence on the rotational capacity. The theoretical analysis does not clearly demonstrate any great influence of this kind. However, Cederwall et al. /4/ report that they have found that a mild strain hardening steel gives much higher rotational capacities than a cold worked steel with a small ratio between ultimate strength and yield strength. This difference can partly be explained by the definition of rotational capacity, discussed above, partly by the plastic curvature outside the localized zone, which is more important for strain hardening steel. Another possible explanation is the difference in bond between different types of reinforcing bars.

CONCLUSIONS

A possible expression for the rotational capacity may be

$$\theta_{pl} = \frac{k}{\omega d} - \frac{f_s}{E_s}$$

where ω may be taken as the difference between the mechanical reinforcement ratios of the tension and compression reinforcements.

The expression shows that the beam depth d is an important parameter.

The expression is only valid if buckling of the compression reinforcement is prevented.

The value k (a length) is primarily a material property, which can be expected to be smaller for high strength concrete and for light weight concrete than for ordinary concrete. The value is also influenced by confinement, e.g. from stirrups.

The type of reinforcement may also be of importance for the rotational capacity. This influence might be included in the value of k, which will then depend also on the type of reinforcing steel.

REFERENCES

1. CEB-FIP Model code for concrete structures (1978), CEB Bulletin 124/125-E.

2. Langer, P., Verdrehfähigkeit plastizierter Tragwerksbereiche im Stahlbetonbau, Mitteilungen, IWB, Universität Stuttgart, 1987/1.

3. Corley, W.G., Rotational capacity of reinforced concrete beams. Journal of the Structural Division, Proc of ASCE, Vol. 92, ST5, 121-146, October 1966. Also PCA Bulletin D108.

4. Cederwall, K., Losberg, A., Palm, G., Armerade betongbalkars rotationskapacitet (Rotational capacity of reinforced concrete beams, in Swedish), Nordisk Betong 4:1974, 9-16.

NOTATIONS

A_s	area of reinforcement
E_s	modulus of elasticity of reinforcement
L_s	length over which the localized deformation is averaged
M	bending moment
b	beam width
d	beam depth
f_c	concrete compressive strength
f_s	yield strength of reinforcement
r_s	radius of curvature
w	additional deformation in the localized damage zone
w_c	value of w when the stress has decreased to zero
x_c	depth of the compression zone
θ	rotation = angle of deformation in a hinge
θ_{pl}	rotational capacity = plastic part of rotation
β^{pl}	ratio used for defining L, Eq. (3)
ϵ	strain
ϵ_1	$w_c/(\beta d)$
σ	stress
ω	(tensile) mechanical reinforcement ratio, Eq. (12)
ω'	compressive mechanical reinforcement ratio
ξ	x/d see Fig. 3